$X(3872) \to J/\psi\pi\gamma$ and $X(3872) \to J/\psi\pi\pi\gamma$ decays

Qi Wu,* Jun-Zhang Wang,† and Shi-Lin Zhu‡
School of Physics and Center of High Energy Physics, Peking University, Beijing 100871, China

(Received 26 December 2022; accepted 13 March 2023; published 4 April 2023)

We study the ρ and ω meson contribution to the radiative decays $X(3872) \to J/\psi\pi\gamma$ and $X(3872) \to J/\psi\pi\pi\gamma$. The $X(3872) \to J/\psi\pi\gamma$ is dominated by the ω meson. As for the $X(3872) \to J/\psi\pi\pi\gamma$, the contributions of the cascade decays through the ρ and ω mesons are strongly suppressed with respect to the diagrams which proceed either through the $\psi(2S)$ or the three body decay of ρ. The branching ratios of $X(3872) \to J/\psi\pi\gamma$ and $X(3872) \to J/\psi\pi\pi\gamma$ are $(8.10^{+3.50}_{-2.88}) \times 10^{-3}$ and $(2.38 \pm 1.06)\%$, which may be accessible by the BESIII and LHCb collaborations. Especially, the $X(3872) \to J/\psi\pi\gamma$ and $X(3872) \to J/\psi\pi^+\pi^-\gamma$ decays can be employed to extract the couplings $g_{X\psi\omega}$ and $g_{X\psi\rho}$, which probe the isoscalar and isovector components of the $X(3872)$ wave function, respectively.

DOI: 10.1103/PhysRevD.107.074002

I. INTRODUCTION

Twenty years ago, a new narrow charmoniumlike state $X(3872)$ was observed in the exclusive decay process $B^+ \to K^+\pi^+\pi^- J/\psi$ by the Belle collaboration [1], which opened a door to the exotic hadron spectroscopy (see Refs. [2–14] for recent reviews). After its discovery, the $X(3872)$ was subsequently confirmed by several other experiments [15–17]. Ten years after its discovery, its spin-parity quantum numbers were finally determined to be $J^{PC} = 1^{++}$ by the LHCb collaboration [18]. No evidence of the charged partner of the $X(3872)$ was found [19].

Since the discovery of $X(3872)$, there have been tremendous efforts to investigate its inner structure experimentally and theoretically. The exotic nature of the $X(3872)$ was embodied in its mass and width, which are listed in Table I. One of the most intriguing features of $X(3872)$ is that its mass almost coincides with the $D^0\bar{D}^{*0}$ threshold. Considering the narrow width of $X(3872)$, it is natural to regard the $X(3872)$ as a $D\bar{D}^*$ hadronic molecule [20–25]. The molecule picture not only explains the coincidence of the mass of the $X(3872)$ with the $D^0\bar{D}^{*0}$ threshold naturally, but it also explains its isospin violation in the $J/\psi\rho$ decay mode [21,26,27]. However, some molecule models meet with difficulties when explaining the following phenomena:

(1) The ratio $\Gamma(B^0 \to K^0 X)/\Gamma(B^+ \to K^+ X)$ is about unity, according to an estimation based on the molecule picture [28–30], which is about two times larger than measurements by the *BABAR* [17] and Belle [31] collaborations.
(2) The predicted branching ratios of $X(3872) \to D^0\bar{D}^0\gamma$ and $X(3872) \to J/\psi\gamma$ [21,26] largely deviated from the experimental data.
(3) As a loosely bound hadronic molecule with a small binding energy, $X(3872)$, was expected to be so fragile that it would be hard to explain the observed production rate in the high energy $p\bar{p}$ collisions at the Tevatron [32].

Actually, the above difficulties indicate that there should exist a significant $c\bar{c}$ component in the wave function of the $X(3872)$ [33,34]. In other words, the coupled channel effect may play an important role in the formation of $X(3872)$.

To date, the inner structure of $X(3872)$ is still an open question and remains challenging. In addition to the mass spectrum, the decay patterns also encode important dynamical information and hence provide another perspective about its underlying structure. The ratio $\mathcal{B}[X \to J/\psi\pi^+\pi^-\pi^0]/\mathcal{B}[X \to J/\psi\pi^+\pi^-]$ has been measured by several experiments [36–38], which indicates a large isospin violation. This ratio is of great interest and has been investigated in different scenarios [22,27,33,39–44]. Different components in the wave function of the $X(3872)$ will affect the decays either in the long distance or the short distance. In other words, the decay patterns encode very important information on the underlying structure and can be used to test different theoretical explanations. For example, $X \to D^0\bar{D}^0\pi/\gamma$, which proceeds through the decays of either D^{*0} or $\bar{D}^{*0}$ and thus belongs to the long-distance decays, can be used to study the long-distance structure of the $X(3872)$ [20]. Pionic

*wu_qi@pku.edu.cn
†wangjzh2022@pku.edu.cn
‡zhusl@pku.edu.cn

TABLE I. The resonance parameters of the $X(3872)$ from Particle Data Group (PDG) [35] (in units of MeV), where $\Delta E = M_X - M_{\text{Threshold}}$.

Mass	Width	Threshold	ΔE
3871.65 ± 0.06	1.19 ± 0.21	$D^+D^{*-}/D^0\bar{D}^{*0}$	$-8/-0.04$

transitions from the $X(3872)$ to χ_{cJ} were investigated in Refs. [45–47]. The relative rates for these transitions to the final states with different J is very sensitive to the inner structure of the $X(3872)$ as a pure charmonium state or a four-quark/molecular state [45]. The predictions of the ratio $\mathcal{B}[X \to \psi'\gamma]/\mathcal{B}[X \to J/\psi\gamma]$ from the $D\bar{D}^*$ molecule [21,48], pure charmonium state [49], and molecule-charmonium mixture [50,51] turned out to be dramatically different from each other, which reflects the importance of the $c\bar{c}$ component in the $X(3872)$.

In order to pin down the nature of the $X(3872)$, searching for more decay modes is crucial. In Table II, we list the observed decays of the $X(3872)$. The dominant decay channel is the open-charm decay, which is 37% for the $D^0\bar{D}^{*0}$ and 49% for the $D^0\bar{D}^0\pi^0$. The branching ratios of the radiative decays $J/\psi\gamma$ and $\psi'\gamma$ are of the same order as those of the hidden-charm decays. Are there other radiative decays of the $X(3872)$ whose decay rates could be as large as those of the $J/\psi\gamma$ and $\psi'\gamma$?.

Recently, the LHCb collaboration observed a sizeable ω contribution to $X(3872) \to J/\psi\pi\pi$ decay [52]. Inspired by the recent LHCb collaboration measurements, we study the ρ and ω meson contributions to the radiative decay processes $X(3872) \to J/\psi\pi\gamma$ and $X(3872) \to J/\psi\pi\pi\gamma$ in this work. In Ref. [53], the authors noted that the dominant contributions to $X(3872) \to J/\psi\pi^+\pi^-$ and $X(3872) \to J/\psi\pi^+\pi^-\pi^0$ arise from the diagrams with the $X(3872)$ coupling to the $J/\psi\rho$ and $J/\psi\omega$, respectively. One may wonder whether the same scenario still holds in the $X(3872) \to J/\psi\pi\gamma$ and $X(3872) \to J/\psi\pi\pi\gamma$.

Compared with $X(3872) \to J/\psi\pi\pi$, $X(3872) \to J/\psi\pi\gamma$ has an advantage in exploring the isospin violation of the $J/\psi\rho$ mode. The LHCb experiment has proved that there is a sizeable ω contribution to $X(3872) \to J/\psi\pi\pi$. In other words, the $X(3872) \to J/\psi\pi\pi$ is not a clean process to

TABLE II. The branching ratios (%) of $X(3872)$ from PDG [35].

Decay channels	Branching ratios
$\pi^+\pi^- J/\psi$	3.8 ± 1.2
$\omega J/\psi$	4.3 ± 2.1
$D^0\bar{D}^0\pi^0$	49^{+18}_{-20}
$D^0\bar{D}^{*0}$	37 ± 9
$\pi^0\chi_{c1}$	3.4 ± 1.6
$\gamma J/\psi$	0.8 ± 0.4
$\gamma\psi(2S)$	4.5 ± 2.0

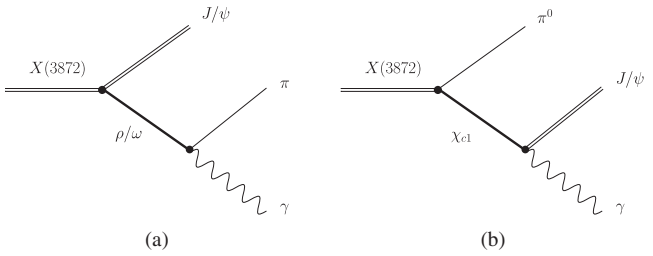

FIG. 1. Diagrams for the $X(3872) \to J/\psi\pi\gamma$ with the ρ^0/ω contribution (a) and χ_{c1} contribution (b).

study the isospin violation of the $J/\psi\rho$ mode. In Fig. 1(a), the $X(3872) \to J/\psi\pi\gamma$ decay occurs through the intermediate ρ or ω meson. The ω meson dominates this process because $g_{X\psi\omega}$ and $g_{\omega\pi\gamma}$ are both much larger than $g_{X\psi\rho}$ and $g_{\rho\pi\gamma}$, respectively. Thus, the $X(3872) \to J/\psi\pi\gamma$ should be a cleaner process to extract the coupling $g_{X\psi\omega}$. By the same token, the $X(3872) \to J/\psi\pi\pi\gamma$ is a cleaner process to study the isospin violation channel of $J/\psi\rho$. For this purpose, we will not only check the contribution of the ρ and ω mesons to the $X(3872) \to J/\psi\pi\gamma$ process but also the contributions of diagrams with the $X(3872)$ coupling to the $J/\psi\rho$ or $J/\psi\omega$ in the $X(3872) \to J/\psi\pi\pi\gamma$ process. Besides the ρ and ω contributions, there are some nonresonant contributions that should be considered as the background contribution. We will predict the branching ratios of $X(3872) \to J/\psi\pi\gamma$ and $X(3872) \to J/\psi\pi\pi\gamma$, which could be tested by the BESIII and LHCb collaborations.

This paper is organized as follows. After the introduction, we present the theoretical framework in the calculation of $X(3872) \to J/\psi\pi\gamma$ and $X(3872) \to J/\psi\pi\pi\gamma$. We derive the invariant decay amplitudes and invariant mass distributions using the effective Lagrangian method. In Sec. III, we present the invariant mass distribution of $\pi\gamma$ and $\pi\pi\gamma$, and the branching ratios of $X(3872) \to J/\psi\pi\gamma$ and $X(3872) \to J/\psi\pi\pi\gamma$. Section IV is a short summary.

II. THEORETICAL FRAMEWORK

In this work, we utilize the effective Lagrangian method to study the radiative processes $X(3872) \to J/\psi\pi\gamma$ and $X(3872) \to J/\psi\pi\pi\gamma$. In the following subsections, we introduce the effective Lagrangian and invariant decay amplitudes and the formulas of the invariant mass distributions related to the radiative processes $X(3872) \to J/\psi\pi\gamma$ and $X(3872) \to J/\psi\pi\pi\gamma$.

A. Feynman diagrams and effective Lagrangian

In Figs. 1(a), 2(a), and 2(b), the decays $X(3872) \to J/\psi\pi\gamma$ and $X(3872) \to J/\psi\pi\pi\gamma$ occur through the ρ and ω as the intermediate states. As shown in Table II, the branching ratios of the decays $X(3872) \to \pi^0\chi_{c1}$ and $X(3872) \to \gamma\psi(2S)$ are sizable. In addition, the branching ratios of $\psi(2S) \to J/\psi\pi^+\pi^-$ and $\psi(2S) \to J/\psi\pi^0\pi^0$ are

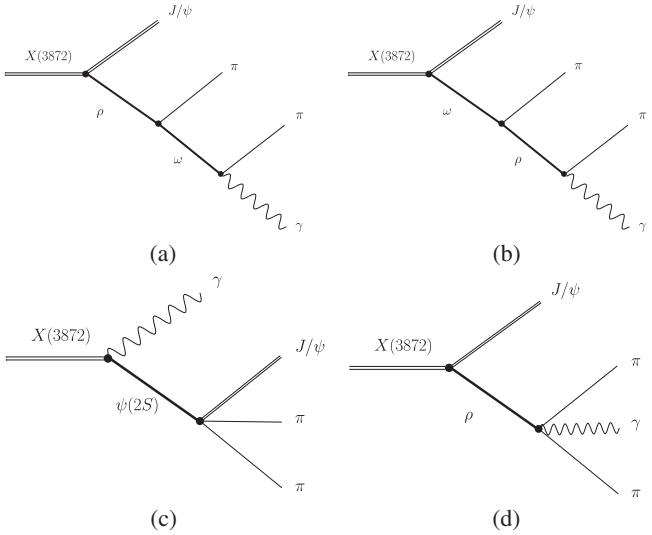

FIG. 2. Diagrams for the $X(3872) \to J/\psi\pi\pi\gamma$ with the $X(3872)$ coupling to the $J/\psi\rho$ (a), $J/\psi\omega$ (b), $\psi(2S)$ (c), and ρ (d), respectively.

$(34.68 \pm 0.30)\%$ and $(18.24 \pm 0.31)\%$ respectively [35]. The branching ratio of the $\chi_{c1} \to \gamma J/\psi$ is also quite large. Thus, the diagrams in Figs. 1(b) and 2(c) will also contribute to the background. In contrast, the $\pi\gamma$ and $\pi\pi\gamma$ invariant mass spectrum tend to peak around the ρ and ω mass for our concerned ρ and ω contributions. Besides, the QED gauge invariance requires the existence of Fig. 2(d). One notes that the ω may also contribute to Fig. 2(d). The branching ratio of $\omega \to \pi^0\pi^0\gamma$ is $(6.7 \pm 1.1) \times 10^{-5}$ [35]. The branching ratio of $\omega \to \pi^+\pi^-\gamma$ has not been measured yet. If one neglects the long range contributions and considers the isospin symmetry, then the branching ratio of $\omega \to \pi^+\pi^-\gamma$ is just twice $\omega \to \pi^0\pi^0\gamma$. In contrast, the branching ratio of $\rho \to \pi^+\pi^-\gamma$ is around 10^{-2}. In other words, the ω contribution to Fig. 2(d) is much smaller than the ρ contribution. Thus, we only consider the diagram in Fig. 2(d).

In order to get the invariant decay amplitudes in Figs. 1 and 2, we need the following effective Lagrangian [54–57],

$$\mathcal{L}_{XJ/\psi V} = g_{X\psi V}\varepsilon^{\mu\nu\alpha\beta}\partial_\mu X_\nu \psi_\alpha V_\beta, \tag{1}$$

$$\mathcal{L}_{X\chi_{c1}\pi} = \frac{g_{X\chi_{c1}\pi}}{m_X}\varepsilon^{\mu\nu\alpha\beta}\partial_\mu X_\nu \chi_{c1\alpha}\partial_\beta \pi, \tag{2}$$

$$\mathcal{L}_{X\psi'\gamma} = g_{X\psi'\gamma}\varepsilon^{\mu\nu\alpha\beta} X_\mu \psi'_\nu \partial_\alpha A^\gamma_\beta, \tag{3}$$

$$\mathcal{L}_{\omega\rho\pi} = g_{\omega\rho\pi}\varepsilon^{\mu\nu\alpha\beta}\partial_\mu \omega_\alpha \partial_\nu \rho_\beta \phi_\pi, \tag{4}$$

$$\mathcal{L}_{V\pi\gamma} = g_{V\pi\gamma}\varepsilon^{\mu\nu\alpha\beta} F_{\mu\nu} V_{\alpha\beta}\phi_\pi, \tag{5}$$

$$\mathcal{L}_{\chi_{c1}\psi\gamma} = g_{\chi_{c1}\psi\gamma}\varepsilon^{\mu\nu\alpha\beta}\partial_\mu \chi_{c1\nu} v^\xi \psi_\alpha F_{\beta\xi}, \tag{6}$$

where X, V, ψ', χ_{c1} stand for $X(3872)$, ρ/ω, $\psi(2S)$, and $\chi_{c1}(1P)$, respectively. $g_{X\psi V}$, $g_{X\chi c1\pi}$, $g_{X\psi'\gamma}$, $g_{\omega\rho\pi}$, $g_{V\pi\gamma}$, and $g_{\chi_{c1}\psi\gamma}$ are the relevant coupling constants and will be discussed in the next subsection. In addition, the electromagnetic field strength tensor is $F_{\mu\nu} = \partial_\mu A^\gamma_\nu - \partial_\nu A^\gamma_\mu$ and $V_{\alpha\beta} = \partial_\alpha V_\beta - \partial_\beta V_\alpha$.

The $\rho \to \pi\pi$ effective Lagrangian reads

$$\mathcal{L}_{\rho\pi\pi} = g_{\rho\pi\pi}\rho_\mu(\phi_{\pi^+} D^{\dagger\mu}\phi_{\pi^-} - \phi_{\pi^-} D^\mu \phi_{\pi^+}), \tag{7}$$

where $D^\mu = \partial^\mu + ieA^\mu$. The $\rho \to \pi\pi\gamma$ vertex arises from the contact seagull interaction, which contributes to Fig. 2(d).

B. Invariant decay amplitudes

With the above effective Lagrangian, the invariant decay amplitudes of $X(p) \to J/\psi(p_1) + \rho(q) \to J/\psi(p_1) + \pi(p_2) + \gamma(p_3)$ shown in Fig. 1(a) is

$$\begin{aligned}\mathcal{M}^{\pi\gamma}_{\rho} = {} & (g_{X\psi\rho}\varepsilon_{\xi\kappa\phi\theta} i p^\xi \epsilon^\kappa(p) p_1^\phi q^\theta)\frac{-g^{\theta\sigma} + q^\theta q^\sigma/m_\rho^2}{D_\rho(q^2)} \\ & \times (g_{\rho\pi\gamma}\varepsilon_{\mu\nu\alpha\beta}(p_3^\mu g^{\rho\nu} - p_3^\nu g^{\rho\mu})(q^\alpha g^{\sigma\beta} - q^\beta g^{\sigma\alpha})\epsilon_\rho(p_3)) \\ & \times F_\rho(q^2),\end{aligned} \tag{8}$$

the invariant decay amplitudes of $X(p) \to \pi(p_2) + \chi_{c1}(q) \to J/\psi(p_1) + \pi(p_2) + \gamma(p_3)$ shown in Fig. 1(b) is

$$\begin{aligned}\mathcal{M}^{\pi\gamma}_{\chi_{c1}} = {} & \left(\frac{g_{X\chi_{c1}\pi}}{m_X}\varepsilon_{\xi\kappa\phi\theta} i p^\xi \epsilon^\kappa(p) i p_2^\theta\right)\frac{-g^{\phi\nu} + q^\phi q^\nu/m_\rho^{\chi_{c1}}}{D_{\chi_{c1}}(q^2)} \\ & \times \left(\frac{\sqrt{2}g_{\chi_{c1}\psi\gamma}}{m_{\chi_{c1}}}\varepsilon_{\mu\nu\alpha\beta}(-i) q^\mu v^\xi \epsilon^\alpha(p_1) i(p_3^\beta \epsilon^\xi(p_3)\right. \\ & \left. - p_3^\xi \epsilon^\beta(p_3))\right) F_{\chi_{c1}}(q^2),\end{aligned} \tag{9}$$

and the invariant decay amplitudes of $X(p) \to J/\psi(p_4) + \pi(p_1) + \pi(p_2) + \gamma(p_3)$ shown in Fig. 2(a) is

$$\begin{aligned}\mathcal{M}^{\pi\pi\gamma}_{\rho} = {} & (g_{X\psi\rho}\varepsilon_{\xi\kappa\phi\theta} i p^\xi \epsilon^\kappa(p)\epsilon^\phi(p_4))\frac{-g^{\theta\eta} + q_1^\theta q_1^\eta/m_\rho^2}{D_\rho(q^2)} \\ & \times (g_{\omega\rho\pi}\varepsilon_{\lambda\omega\delta\eta} q_2^\lambda q_1^\omega)\frac{-g^{\delta\sigma} + q_2^\delta q_2^\sigma/m_\omega^2}{D_\omega(q_2^2)} \\ & \times (g_{\omega\pi\gamma}\varepsilon_{\mu\nu\alpha\beta}\epsilon_\rho(p_3)(p_3^\mu g^{\rho\nu} - p_3^\nu g^{\rho\mu})(q_2^\alpha g^{\sigma\beta} - q_2^\beta g^{\sigma\alpha})) \\ & \times F_\rho(q_1^2) F_\omega(q_2^2),\end{aligned} \tag{10}$$

where p, p_1, p_2, p_3, p_4 are the four-momenta of $X(3872)$, π^-, π^+, γ, J/ψ, while q_1 and q_2 represent the four-momenta of the intermediate ρ^0 and ω mesons. $D_\rho(q^2)$ and $D_\omega(q_1^2)$ are the denominators of the propagators for the ρ and ω meson, which are

$$D_\rho(q_1^2) = q_1^2 - m_\rho^2 + i m_\rho \Gamma_\rho, \tag{11}$$

$$D_\omega(q_2^2) = q_2^2 - m_\omega^2 + i m_\omega \Gamma_\omega. \tag{12}$$

Here, the ρ meson is not far away from its mass shell and the width of the ω meson is narrow enough that its energy dependence can be safely neglected. Thus, we take the $\Gamma_{\rho/\omega}$ as a constant.

The invariant decay amplitudes of $X(3872) \to J/\psi\omega \to J/\psi\pi\gamma$ in Fig. 1(a) and $X(3872) \to J/\psi\pi\pi\gamma$ in Fig. 2(b) can be obtained by

$$\begin{aligned}\mathcal{M}_\omega^{\pi\gamma} &= \mathcal{M}_\rho^{\pi\gamma}|_{g_{X\psi\rho}\to g_{X\psi\omega}, g_{\rho\pi\gamma}\to g_{\omega\pi\gamma}, m_\rho \to m_\omega},\\ \mathcal{M}_\omega^{\pi\pi\gamma} &= \mathcal{M}_\rho^{\pi\pi\gamma}|_{g_{X\psi\rho}\to g_{X\psi\omega}, g_{\omega\pi\gamma}\to g_{\rho\pi\gamma}, m_\rho \leftrightarrow m_\omega}.\end{aligned} \tag{13}$$

In evaluating the decay amplitudes of $X(3872) \to J/\psi\pi\gamma$ and $X(3872) \to J/\psi\pi\pi\gamma$ associated with the ρ and ω mesons in Figs. 1 and 2, we include the form factors for the ρ and ω mesons since they are not pointlike particles [58]. In this work we adopt the following form factor:

$$F_{\rho/\omega}(q^2) = \frac{\Lambda_{\rho/\omega}^4}{\Lambda_{\rho/\omega}^4 + (q^2 - m_{\rho/\omega}^2)^2}, \tag{14}$$

where we adopt $\Lambda_\rho = \Lambda_\omega = 598$ MeV as a result of Γ_ρ being a constant [53]. We have checked that our results barely depend on the form factor.

In Ref. [53], the coupling constants $g_{X\psi\rho}$ and $g_{X\psi\omega}$ are determined to be 0.09 ± 0.02 and 0.31 ± 0.06 by fitting to the LHCb data with Γ_ρ being a constant. Other coupling constants can be determined from the corresponding experimental partial widths. With the effective Lagrangian in Eqs. (2)–(6), the decay widths of $\rho \to \pi\gamma$, $\omega \to \pi\gamma$, $X(3872) \to \psi(2S)\gamma$, $X(3872) \to \chi_{c1}\pi$, and $\chi_{c1} \to J/\psi\gamma$ are

$$\Gamma_{\rho\to\pi\gamma} = \frac{4 g_{\rho\pi\gamma}^2 p_{f\rho}^3}{3\pi}, \tag{15}$$

$$\Gamma_{\omega\to\pi\gamma} = \frac{4 g_{\omega\pi\gamma}^2 p_{f\omega}^3}{3\pi}, \tag{16}$$

$$\Gamma_{X\to\psi'\gamma} = \frac{g_{X\psi'\gamma}^2 p_{fX}^3}{12\pi m_X^2 m_{\psi'}^2}(m_X^2 + m_{\psi'}^2), \tag{17}$$

$$\Gamma_{X\to\chi_{c1}\pi} = \frac{g_{X\psi'\gamma}^2 p_{fX}^3}{12\pi m_X^2}, \tag{18}$$

$$\Gamma_{\chi_{c1}\to J/\psi\gamma} = \frac{g_{\chi_{c1}\psi\gamma}^2 p_{f\chi_{c1}}^3 m_\psi}{3\pi m_{\chi_{c1}}}, \tag{19}$$

where $p_{f\rho}$, $p_{f\omega}$, p_{fX}, and $p_{f\chi_{c1}}$ are the three-momenta of the final mesons in the ρ, ω, $X(3872)$, and χ_{c1} rest frame, respectively. With $\mathcal{B}[\rho^0 \to \pi^0\gamma] = 4.7 \times 10^{-4}$, $\mathcal{B}[\omega \to \pi^0\gamma] = 8.35\%$, $\mathcal{B}[X(3872) \to \psi'\gamma] = 4.5\%$, and $\mathcal{B}[X(3872) \to \chi_{c1}\pi] = 3.4\%$, we have $|g_{\rho\pi\gamma}| = 0.06$ GeV^{-1}, $|g_{\omega\pi\gamma}| = 0.18$ GeV^{-1}, $|g_{X\psi'\gamma}| = 1.56$, and $|g_{X\chi c1\pi}| = 0.84^{+0.18}_{-0.23}$. $g_{\chi_{c1}\psi\gamma} = \sqrt{\frac{2m_\psi}{m_{\chi_{c1}}}} g_{PS\gamma}$ and $|g_{PS\gamma}| = 0.23$ GeV^{-1}. $g_{\omega\rho\pi}$ can be determined from the experimentally measured partial decay of $\omega \to \rho\pi \to \pi\pi\pi$, which is $|g_{\omega\rho\pi}| = 50$ GeV^{-1} with Γ_ρ being a constant [53]. Note that one can only obtain the absolute value of the coupling constant from the partial decay width. The phase cannot be fixed. In this work, the default values of the above coupling constants are real and positive.

The total invariant decay amplitudes of $X(3872) \to J/\psi\pi\gamma$ and $X(3872) \to J/\psi\pi\pi\gamma$ are

$$\begin{aligned}\mathcal{M}_{X\to J/\psi\pi\gamma} &= \mathcal{M}_\rho^{\pi\gamma} + e^{i\phi_\omega}\mathcal{M}_\omega^{\pi\gamma} + e^{i\phi_{\chi_{c1}}}\mathcal{M}_{\chi_{c1}}^{\pi\gamma},\\ \mathcal{M}_{X\to J/\psi\pi\pi\gamma} &= \mathcal{M}_\rho^{\pi\pi\gamma} + e^{i\phi_\omega}\mathcal{M}_\omega^{\pi\pi\gamma} + e^{i\phi_{\psi'}}\mathcal{M}_{\psi'}^{\pi\pi\gamma},\end{aligned} \tag{20}$$

where ϕ_ω stands for the relative phase between the ω and ρ terms, $\phi_{\psi'}$ stands for the relative phase between ρ/ω and ψ' terms. We adopt the phase angle ϕ_ω obtained by fitting the LHCb data in Ref. [53], which is 134.5°.

C. Invariant mass distributions

The invariant $\pi^0\gamma$ mass distribution of the $X(3872) \to J/\psi\pi^0\gamma$ decay is given by

$$\frac{d\Gamma_{X3872\to J/\psi\pi^0\gamma}}{dM_{\pi^0\gamma}} = \frac{1}{24(2\pi)^4 M_X^2} \times \int \Sigma|\mathcal{M}_{\pi\gamma}|^2 |\mathbf{p}_1^*||\mathbf{p}_4| d\cos\theta_1 d\phi_1, \tag{21}$$

where $\mathbf{p}_1^*$ and (θ_1, ϕ_1) are the three-momentum and decay angle of the outgoing π^0/γ in the c.m. frame of the final $\pi^0\gamma$ system, $\mathbf{p}_4$ is the three-momentum of the final J/ψ meson in the rest frame of $X(3872)$, and $M_{\pi^0\gamma}$ is the invariant mass of the final $\pi^0\gamma$ system.

For the invariant $\pi\pi\gamma$ mass distributions of the $X(3872) \to J/\psi\pi\pi\gamma$ decay,

$$\begin{aligned}&\frac{d\Gamma_{X(3872)\to J/\psi\pi\pi\gamma}}{dM_{\pi\pi\gamma}}\\ &= \frac{1}{16(2\pi)^7 M_X^2}\int \Sigma|\mathcal{M}_{\pi\pi\gamma}|^2\\ &\quad\times |\mathbf{p}_1^*||\mathbf{p}_3'||\mathbf{p}_4| dM_{\pi\gamma} d\cos\theta_1 d\phi_1 d\cos\theta_2 d\phi_2,\end{aligned} \tag{22}$$

with $M_{\pi\pi\gamma}$ the invariant mass of $\pi\pi\gamma$ system. The $\mathbf{p}_1^*$ and (θ_1, ϕ_1) are the three-momentum and decay angles of the outgoing π in the $\pi\gamma$ c.m. frame. The $\mathbf{p}_3'$ and (θ_2, ϕ_2) are the three-momentum and decay angles of the outing π^0 in the $\pi\pi\gamma$ c.m. frame. The $\mathbf{p}_4$ is the three-momentum of the

final J/ψ meson in the $X(3872)$ rest frame. Definitions of these variables in the phase space integration of the $X(3872) \to J/\psi\pi\pi\gamma$ decay can be found in the Appendix of Ref. [53].

III. NUMERICAL RESULTS AND DISCUSSION

A. $X(3872) \to J/\psi\pi\gamma$

In this work, we assume that the phase angle ϕ_ω in $X(3872) \to J/\psi\pi\gamma$ is the same as in the $X(3872) \to J/\psi\pi\pi$. Unfortunately, due to the absence of the experimental data, the other phase $\phi_{\chi_{c1}}$ is unknown. We first investigate the $\phi_{\chi_{c1}}$ dependence of the interference term by setting the $m_{\pi\gamma} = 0.5$ GeV, which is shown in Fig. 3. One can see that the interference term is not drastically dependent on the $\phi_{\chi_{c1}}$. Thus it is reasonable to choose the phase angle $\phi_{\chi_{c1}} = 223°$ to estimate the invariant mass distribution of $\pi\gamma$ for the $X(3872) \to J/\psi\pi\gamma$, which corresponds to the central value of the interference term.

In Fig. 4, we present the invariant mass distribution of $\pi\gamma$ for the $X(3872) \to J/\psi\pi\gamma$, when the ϕ_ω and $\phi_{\chi_{c1}}$ are both fixed. Different from the $X(3872) \to J/\psi\pi\pi$ in Ref. [53], which is dominated by the ρ meson, the decay of $X(3872) \to J/\psi\pi\gamma$ is dominated by the ω meson. The line shape of the ω contribution and the total contribution are almost coincident in the high invariant mass region. The differential decay rate with respect to $\pi\gamma$ from the ω contribution is two orders of magnitude larger than that from the ρ meson since $g_{X\psi\omega}$ and $g_{\omega\pi\gamma}$ are both three times larger than $g_{X\psi\rho}$ and $g_{\rho\pi\gamma}$, respectively. Thus, the dominant resonance contribution of $X(3872) \to J/\psi\pi\gamma$ is the ω meson. The χ_{c1} term provides the dominant the nonresonance contribution, which serves as the background. Due to the absolute dominance of the ω in $X(3872) \to J/\psi\pi\gamma$, $X(3872) \to J/\psi\pi\gamma$ becomes a clean and ideal process to explore the isospin conservation channel $J/\psi\omega$ of $X(3872)$. In the line shape of the total invariant mass distribution, there is a dip around 766 MeV, which results from the dip of the interference term. After integrating over the $\pi\gamma$ invariant mass, the branching ratio of $X(3872) \to J/\psi\pi\gamma$ is $(8.10^{+3.44}_{-2.84}) \times 10^{-3}$ considering the ρ and ω contributions only.

The above branching ratio does not include the contribution from the χ_{c1} term. To gain the total branching ratio of $X(3872) \to J/\psi\pi\gamma$ including the χ_{c1} term, the $\phi_{\chi_{c1}}$ dependence of the total branching ratio of $X(3872) \to J/\psi\pi\gamma$ should be clarified.

In Fig. 5, we present the $\phi_{\chi_{c1}}$ dependence of the total branching ratio of $X(3872) \to J/\psi\pi\gamma$ by fixing the ϕ_ω to be 134.5° and varying the $\phi_{\chi_{c1}}$ from 0° to 360°. The $\phi_{\chi_{c1}}$ dependence of the total branching ratio of $X(3872) \to J/\psi\pi\gamma$ is fairly stable. Finally, the predicted branching ratio of $X(3872) \to J/\psi\pi\gamma$ is $(8.10^{+3.59}_{-2.89}) \times 10^{-3}$. The central value is obtained by taking $\phi_{\chi_{c1}} = 180°$, the errors come from the variation of the $\phi_{\chi_{c1}}$. Under the assumption that $X(3872)$ is a $D\bar{D}^*$ molecule and that its decay proceeds through the transitions to $J/\psi\rho$ and $J/\psi\omega$, the branching ratio of $X(3872) \to J/\psi\pi\gamma$ was estimated to be $0.17 \times \mathcal{B}[X \to J/\psi\pi\pi]$ [59], which is similar to our estimation. Our results indicate that the branching ratio of $X(3872) \to J/\psi\pi\gamma$ is almost of the same order as those of the hidden-charm and radiative decays to $\psi'/J/\psi$ of the $X(3872)$, which is large enough to be detected experimentally.

B. $X(3872) \to J/\psi\pi\pi\gamma$

In the hidden charm decay of $X(3872) \to J/\psi\pi\pi\pi$, the coupling constants $g_{X\psi\omega}$ and $g_{\rho\pi\pi}$ are both larger than $g_{X\psi\rho}$ and $g_{\omega\pi\pi}$ respectively. As a result, the diagram where the

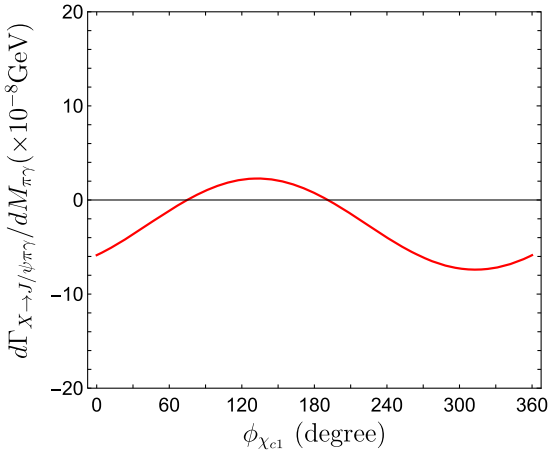

FIG. 3. The $\phi_{\chi_{c1}}$ dependence of the invariant mass distribution of $\pi\gamma$ for the $X(3872) \to J/\psi\pi\gamma$ by considering the interference term with $m_{\pi\gamma} = 0.5$ GeV.

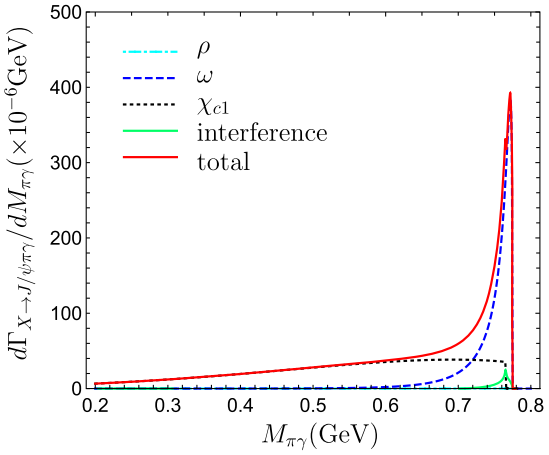

FIG. 4. Invariant mass distribution of $\pi\gamma$ for the $X(3872) \to J/\psi\pi\gamma$. The blue-dash-dotted, blue-dashed, black-dashed, and green and red solid lines are the ρ, ω, χ_{c1}, interference term, and total contribution, respectively.

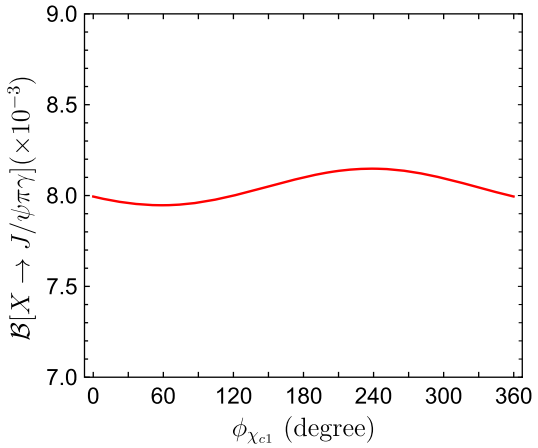

FIG. 5. The $\phi_{\chi_{c1}}$ dependence of the total branching ratio of $X(3872) \to J/\psi\pi\gamma$.

$X(3872)$ couples to $J/\psi\omega$ is far more important than the diagram where the $X(3872)$ couples to the $J/\psi\rho$ [53].

For the radiative decay of $X(3872) \to J/\psi\pi\pi\gamma$, $g_{X\psi\omega}$ is larger than $g_{X\psi\rho}$, while $g_{\rho\pi\gamma}$ is smaller than $g_{\omega\pi\gamma}$ as shown in Figs. 2(a) and 2(b). Thus, the contribution of Fig. 2(a) is probably comparable to that of Fig. 2(b). Here, it should be noted that Fig. 2(a) only contributes to the $X(3872) \to J/\psi\pi^0\pi^0\gamma$ process. In Fig. 6, we show the results of the $\pi\pi\gamma$ invariant mass spectrum based on the contributions of Figs. 2(a) and 2(b), which are governed by the $J/\psi\rho$ and $J/\psi\omega$ coupling, respectively. It can be seen that the contribution of the $J/\psi\omega$ channel is still larger than that of the $J/\psi\rho$ channel. After integrating over the $\pi\pi\gamma$ invariant mass, the branching

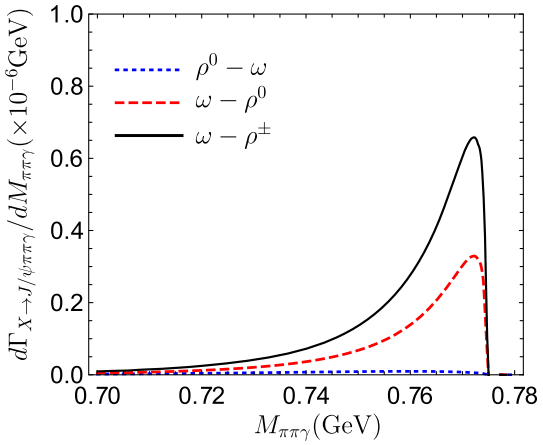

FIG. 6. Invariant mass distribution of $\pi\pi\gamma$ for the $X(3872) \to J/\psi\pi\pi\gamma$. The blue-dotted stands for $X(3872) \to J/\psi\pi^0\pi^0\gamma$ with the intermediate states $\rho^0 - \omega$. The red-dashed and black-solid stand for $X(3872) \to J/\psi\pi^0\pi^0\gamma$ and $X(3872) \to J/\psi\pi^+\pi^-\gamma$ with the intermediate states $\omega - \rho^0$ and $\omega - \rho^\pm$, respectively.

ratios of $X(3872) \to J/\psi\pi^0\pi^0\gamma$ are $(3.84^{+1.90}_{-1.52}) \times 10^{-7}$ for Fig. 2(a) and $(4.58^{+1.94}_{-1.60}) \times 10^{-6}$ for Fig. 2(b).

In addition to Figs. 2(a) and 2(b), the diagram in Fig. 2(c) could also contribute to $X(3872) \to J/\psi\pi\pi\gamma$. The intermediate state $\psi(2S)$ is so narrow that we can use the narrow width approximation to estimate its contribution, which is $\mathcal{B}[X(3872) \to \gamma\psi(2S) \to \gamma J/\psi\pi\pi] \simeq \mathcal{B}[X(3872) \to \gamma\psi(2S)] \times \mathcal{B}[\psi(2S) \to J/\psi\pi\pi]$. Using $\mathcal{B}[X(3872) \to \gamma\psi(2S)] = (4.5 \pm 2.0)\%$ and $\mathcal{B}[\psi' \to J/\psi\pi^0\pi^0] = (18.24 \pm 0.31)\%$ given by PDG [35], the branching ratios of $X(3872) \to \gamma\psi' \to \gamma J/\psi\pi^0\pi^0$ is $(0.82 \pm 0.37)\%$.

As for the direct coupling diagram in Fig. 2(d), the intermediate ρ meson is almost on shell with a large width. Since the threshold of $J/\psi\rho$ is very close to the mass of $X(3872)$, it is a good approximation to write the decay width of $X(3872) \to \rho J/\psi \to J/\psi\pi\pi\gamma$ as

$$\Gamma_{X\to J/\psi\rho\to J/\psi\pi\pi\gamma} = \int_{(2m_\pi)^2}^{(m_X-m_{J/\psi})^2} ds f(s, m_\rho, \Gamma_\rho) \times \frac{|\vec{p}|}{24\pi m_X^2} \overline{|\mathcal{M}^{\text{tot}}_{X\to J/\psi\rho}(m_\rho \to \sqrt{s})|^2} \times \mathcal{B}[\rho \to \pi\pi\gamma], \tag{23}$$

which is equivalent to the Appendix of Ref. [44]. $f(s, m_\rho, \Gamma_\rho)$ is a relativistic form of the Breit-Wigner distribution, which reads

$$f(s, m_\rho, \Gamma_\rho) = \frac{1}{\pi} \frac{m_\rho \Gamma_\rho}{(s - m_\rho^2)^2 + m_\rho^2 \Gamma_\rho^2}, \tag{24}$$

and the amplitude $\mathcal{M}^{\text{tot}}_{X(3872)\to J/\psi\rho}(m_\rho \to \sqrt{s})$ can be obtained by replacing the ρ meson mass by $\sqrt{s}$. In the same way the momentum of the final state becomes

$$|\vec{p}| = \frac{\sqrt{[m_X^2 - (\sqrt{s} - m_{J/\psi})^2][m_X^2 - (\sqrt{s} + m_{J/\psi})^2]}}{2m_X}. \tag{25}$$

The invariant mass distribution of $\pi\pi\gamma$ for the $X(3872) \to \rho J/\psi \to J/\psi\pi\pi\gamma$ decay is

$$\frac{d\Gamma_{X\to J/\psi\rho\to J/\psi\pi\pi\gamma}}{ds} = f(s, m_\rho, \Gamma_\rho) \times \frac{|\vec{p}|}{24\pi m_X^2} \overline{|\mathcal{M}^{\text{tot}}_{X\to J/\psi\rho}(m_\rho \to \sqrt{s})|^2} \times \mathcal{B}[\rho \to \pi\pi\gamma]. \tag{26}$$

The branching ratios of $\rho \to \pi^+\pi^-\gamma$ and $\rho \to \pi^0\pi^0\gamma$ are $(9.9 \pm 1.6) \times 10^{-3}$ and $(4.5 \pm 0.8) \times 10^{-5}$ [35], respectively. In this way, the branching ratio of $X(3872) \to J/\psi\rho \to J/\psi\pi^0\pi^0\gamma$ is $(2.07 \pm 0.52) \times 10^{-6}$.

Now we discuss the $X(3872) \to J/\psi\pi^+\pi^-\gamma$. After integrating over the $\pi\pi\gamma$ invariant mass, the branching ratio

of $X(3872) \to J/\psi\omega \to J/\psi\pi^+\pi^-\gamma$ are $(9.16^{+3.89}_{-3.20}) \times 10^{-6}$ for Fig. 2(b). Using the narrow width approximation and $\mathcal{B}[\psi' \to J/\psi\pi^+\pi^-] = (34.68 \pm 0.30)\%$ [35], the contribution of Fig. 2(c) is $\mathcal{B}[X(3872) \to \gamma\psi(2S) \to \gamma J/\psi\pi^+\pi^-] \simeq \mathcal{B}[X(3872) \to \gamma\psi(2S)] \times \mathcal{B}[\psi(2S) \to J/\psi\pi^+\pi^-] = (1.56 \pm 0.69)\%$.

With Eqs. (23)–(26), the branching ratio of $X(3872) \to J/\psi\rho \to J/\psi\pi^+\pi^-\gamma$ is estimated to be $(4.55 \pm 1.09) \times 10^{-4}$ for Fig. 2(d). In addition to the important background contribution of $X(3872) \to \gamma\psi' \to \gamma J/\psi\pi\pi$, the $J/\psi\rho$ channel contribution is far larger than that of the $J/\psi\omega$ channel in the $X(3872) \to J/\psi\pi^+\pi^-\gamma$. In other words, the radiative transition of $X(3872) \to J/\psi\pi^+\pi^-\gamma$ is a very clean process to precisely study the isospin violation property of $X(3872)$.

In the present estimation, all the involved coupling constants are extracted from the corresponding experimental data. Thus, one should get the same results regardless of the molecular or other scenarios for the $X(3872)$. On the other hand, the $X(3872) \to J/\psi\pi\gamma$ and $X(3872) \to J/\psi\pi\pi\gamma$ decays are very helpful for constraining the coupling constants $g_{X\psi\rho}$ and $g_{X\psi\omega}$,

$$\begin{aligned}
&\mathcal{B}[X \to J/\psi\pi\gamma] \\
&= 0.002 g^2_{X\psi\rho} + 0.083 g^2_{X\psi\omega} + 0.004 g_{X\psi\rho} g_{X\psi\omega} + 0.012, \\
&\mathcal{B}[X \to J/\psi\pi^0\pi^0\gamma], \\
&= (3.03 \pm 1.16) \times 10^{-4} g^2_{X\psi\rho} + (4.77 \times 10^{-5}) g^2_{X\psi\omega} \\
&\quad + (0.82 \pm 0.37)\%, \\
&\mathcal{B}[X \to J/\psi\pi^+\pi^-\gamma], \\
&= (5.62 \pm 2.22) \times 10^{-2} g^2_{X\psi\rho} + (9.53 \times 10^{-5}) g^2_{X\psi\omega} \\
&\quad + (1.56 \pm 0.69)\%. \qquad (27)
\end{aligned}$$

Note that we have assumed that the interference of the diagrams in Fig. 2 is negligible. From $\mathcal{B}[X \to J/\psi\pi\gamma]$, the coefficient of $g^2_{X\psi\omega}$ is so large that we can easily extract the coupling of $X\psi\omega$ in $X \to J/\psi\omega \to J/\psi\pi\gamma$. The coefficients of $g^2_{X\psi\rho}$ and $g^2_{X\psi\omega}$ in $\mathcal{B}[X \to J/\psi\pi^0\pi^0\gamma]$ are pretty small and thus it is difficult to obtain any useful information about these couplings in $X \to J/\psi\pi^0\pi^0\gamma$. In contrast, it is very interesting to see that the coefficient of $g^2_{X\psi\rho}$ in $\mathcal{B}[X \to J/\psi\pi^+\pi^-\gamma]$ is very large. Thus $X \to J/\psi\pi^+\pi^-\gamma$ is a very good process to extract the coupling $X\psi\rho$. We look forward to the measurement of the branching ratios of $X(3872) \to J/\psi\pi\gamma$ and $X(3872) \to J/\psi\pi\pi\gamma$ in the near future. At that time, not only the predicted branching ratios can be tested but also the coupling constants $g_{X\psi\rho}$ and $g_{X\psi\omega}$ can be extracted.

IV. SUMMARY

As the first established charmoniumlike state, $X(3872)$ is one of the best studied exotic hadron states both experimentally and theoretically. Since its discovery, the mass spectrum, decay behaviors and production mechanism of the $X(3872)$ have been studied extensively. The $D\bar{D}^*$ hadronic molecule is the most popular explanation, with which most of the phenomena related to $X(3872)$ could be best explained. However, the other interpretations cannot be easily ruled out.

In this work, we have studied the ρ and ω meson contribution to the radiative decays $X(3872) \to J/\psi\pi\gamma$ and $X(3872) \to J/\psi\pi\pi\gamma$ using an effective Lagrangian method. We obtain the invariant decay amplitudes of the possible diagrams that contribute to $X(3872) \to J/\psi\pi\gamma$ and $X(3872) \to J/\psi\pi\pi\gamma$. We first investigate the $\phi_{\chi_{c1}}$ dependence of the interference term in $X(3872) \to J/\psi\pi\gamma$, which is not drastic. Thus, we choose a central value of $\phi_{\chi_{c1}}$ to analyze the invariant mass distribution of $\pi\gamma$ for $X(3872) \to J/\psi\pi\gamma$. The total branching ratio of $X(3872) \to J/\psi\pi\gamma$ reaches $(8.10^{+3.59}_{-2.89}) \times 10^{-3}$, which barely depends on $\phi_{\chi_{c1}}$.

Although the ρ meson contribution is dominant in $X(3872) \to J/\psi\pi\pi$, the ω contribution is also sizable as recently measured by the LHCb collaboration [52]. Our numerical results strongly indicate that the $X(3872) \to J/\psi\pi\gamma$ is dominated by the ω meson. Compared with $X(3872) \to J/\psi\pi\pi$, $X(3872) \to J/\psi\pi\gamma$ is an ideal place to extract the coupling of $X(3872)$ with $J/\psi\omega$, which probes the isoscalar component of the $X(3872)$.

As for the $X(3872) \to J/\psi\pi\pi\gamma$ cascade decays, the $J/\psi\omega$ contribution is much more important than that of the $J/\psi\rho$, which is similar to the case of $X(3872) \to J/\psi\pi\pi\pi$. The branching ratios of $X(3872) \to J/\psi\pi\pi\gamma$ with the ρ and ω contribution are in order of 10^{-7}–10^{-6}. However, the contributions of the above cascade decays through the ρ and ω mesons are strongly suppressed with respect to the diagrams which proceed either through the $\psi(2S)$ in Fig. 2(c) or the three body decay of the ρ meson in Fig. 2(d). The QED gauge invariance demands the existence of the seagull diagram Fig. 2(d). The branching ratio of $X(3872) \to J/\psi\rho \to J/\psi\pi^+\pi^-\gamma$ may reach 10^{-4}. The radiative transition of $X(3872) \to J/\psi\pi^+\pi^-\gamma$ seems to be a very clean process to precisely study the isospin violation property of $X(3872)$ and extract the coupling of $X(3872)$ with $J/\psi\rho$, which probes the isovector component of the $X(3872)$.

The branching ratios of $X(3872) \to J/\psi\pi\gamma$ and $X(3872) \to J/\psi\pi\pi\gamma$ are accessible for the BESIII and LHCb collaborations. With the relationships between the branching ratios of $X(3872) \to J/\psi\pi(\pi)\gamma$ and the coupling constants $g_{X\psi\rho/\omega}$, we can extract $g_{X\psi\rho}$ and $g_{X\psi\omega}$ if the branching ratios of $X(3872) \to J/\psi\pi\gamma$ and $X(3872) \to J/\psi\pi\pi\gamma$ are measured in the near future. These couplings encode very important information on the inner structure of the $X(3872)$.

ACKNOWLEDGMENTS

We are grateful to the helpful discussions with Yan-Ke Chen and Bo-Lin Huang. This research is supported by the National Science Foundation of China under Grants No. 11975033, No. 12070131001, and No. 12147168. J.-Z. W. is also supported by the National Postdoctoral Program for Innovative Talent.

[1] S. K. Choi *et al.* (Belle Collaboration), Phys. Rev. Lett. **91**, 262001 (2003).
[2] H.-X. Chen, W. Chen, X. Liu, and S.-L. Zhu, Phys. Rep. **639**, 1 (2016).
[3] A. Hosaka, T. Iijima, K. Miyabayashi, Y. Sakai, and S. Yasui, Prog. Theor. Exp. Phys. **2016**, 062C01 (2016).
[4] R. F. Lebed, R. E. Mitchell, and E. S. Swanson, Prog. Part. Nucl. Phys. **93**, 143 (2017).
[5] A. Esposito, A. Pilloni, and A. D. Polosa, Phys. Rep. **668**, 1 (2016).
[6] F.-K. Guo, C. Hanhart, U.-G. Meißner, Q. Wang, Q. Zhao, and B.-S. Zou, Rev. Mod. Phys. **90**, 015004 (2018).
[7] A. Ali, J. S. Lange, and S. Stone, Prog. Part. Nucl. Phys. **97**, 123 (2017).
[8] S. L. Olsen, T. Skwarnicki, and D. Zieminska, Rev. Mod. Phys. **90**, 015003 (2018).
[9] M. Karliner, J. L. Rosner, and T. Skwarnicki, Annu. Rev. Nucl. Part. Sci. **68**, 17 (2018).
[10] C.-Z. Yuan, Int. J. Mod. Phys. A **33**, 1830018 (2018).
[11] Y. Dong, A. Faessler, and V. E. Lyubovitskij, Prog. Part. Nucl. Phys. **94**, 282 (2017).
[12] Y. R. Liu, H. X. Chen, W. Chen, X. Liu, and S. L. Zhu, Prog. Part. Nucl. Phys. **107**, 237 (2019).
[13] H. X. Chen, W. Chen, X. Liu, Y. R. Liu, and S. L. Zhu, Rep. Prog. Phys. **86**, 026201 (2023).
[14] L. Meng, B. Wang, G. J. Wang, and S. L. Zhu, arXiv:2204.08716.
[15] D. Acosta *et al.* (CDF Collaboration), Phys. Rev. Lett. **93**, 072001 (2004).
[16] V. M. Abazov *et al.* (D0 Collaboration), Phys. Rev. Lett. **93**, 162002 (2004).
[17] B. Aubert (*BABAR* Collaboration), Phys. Rev. D **71**, 071103 (2005).
[18] R. Aaij *et al.* (LHCb Collaboration), Phys. Rev. D **92**, 011102 (2015).
[19] B. Aubert *et al.* (*BABAR* Collaboration), Phys. Rev. D **71**, 031501 (2005).
[20] M. B. Voloshin, Phys. Lett. B **579**, 316 (2004).
[21] E. S. Swanson, Phys. Lett. B **588**, 189 (2004).
[22] N. A. Tornqvist, Phys. Lett. B **590**, 209 (2004).
[23] S. Fleming, M. Kusunoki, T. Mehen, and U. van Kolck, Phys. Rev. D **76**, 034006 (2007).
[24] Y. R. Liu, X. Liu, W. Z. Deng, and S. L. Zhu, Eur. Phys. J. C **56**, 63 (2008).
[25] N. A. Tornqvist, Z. Phys. C **61**, 525 (1994).
[26] E. S. Swanson, Phys. Lett. B **598**, 197 (2004).
[27] N. Li and S. L. Zhu, Phys. Rev. D **86**, 074022 (2012).
[28] E. Braaten and M. Lu, Phys. Rev. D **76**, 094028 (2007).
[29] E. Braaten and M. Lu, Phys. Rev. D **77**, 014029 (2008).
[30] E. Braaten and M. Kusunoki, Phys. Rev. D **69**, 074005 (2004).
[31] S. K. Choi *et al.* (Belle Collaboration), Phys. Rev. D **84**, 052004 (2011).
[32] C. Bignamini, B. Grinstein, F. Piccinini, A. D. Polosa, and C. Sabelli, Phys. Rev. Lett. **103**, 162001 (2009).
[33] M. Suzuki, Phys. Rev. D **72**, 114013 (2005).
[34] B. Q. Li and K. T. Chao, Phys. Rev. D **79**, 094004 (2009).
[35] R. L. Workman *et al.* (Particle Data Group), Prog. Theor. Exp. Phys. **2022**, 083C01 (2022).
[36] K. Abe *et al.* (Belle Collaboration), arXiv:hep-ex/0505037.
[37] P. del Amo Sanchez *et al.* (*BABAR* Collaboration), Phys. Rev. D **82**, 011101 (2010).
[38] M. Ablikim *et al.* (BESIII Collaboration), Phys. Rev. Lett. **122**, 232002 (2019).
[39] P. G. Ortega, J. Segovia, D. R. Entem, and F. Fernandez, Phys. Rev. D **81**, 054023 (2010).
[40] D. Gamermann and E. Oset, Phys. Rev. D **80**, 014003 (2009).
[41] C. Hanhart, Y. S. Kalashnikova, A. E. Kudryavtsev, and A. V. Nefediev, Phys. Rev. D **85**, 011501 (2012).
[42] Z. Y. Zhou and Z. Xiao, Phys. Rev. D **97**, 034011 (2018).
[43] Q. Wu, D. Y. Chen, and T. Matsuki, Eur. Phys. J. C **81**, 193 (2021).
[44] L. Meng, G. J. Wang, B. Wang, and S. L. Zhu, Phys. Rev. D **104**, 094003 (2021).
[45] S. Dubynskiy and M. B. Voloshin, Phys. Rev. D **77**, 014013 (2008).
[46] S. Fleming and T. Mehen, Phys. Rev. D **78**, 094019 (2008).
[47] T. Mehen, Phys. Rev. D **92**, 034019 (2015).
[48] J. Ferretti, G. Galatà, and E. Santopinto, Phys. Rev. D **90**, 054010 (2014).
[49] T. Barnes, S. Godfrey, and E. S. Swanson, Phys. Rev. D **72**, 054026 (2005).
[50] A. M. Badalian, V. D. Orlovsky, Y. A. Simonov, and B. L. G. Bakker, Phys. Rev. D **85**, 114002 (2012).
[51] Y. Dong, A. Faessler, T. Gutsche, and V. E. Lyubovitskij, J. Phys. G **38**, 015001 (2011).
[52] LHCb Collaboration, arXiv:2204.12597.
[53] H. N. Wang, Q. Wang, and J. J. Xie, Phys. Rev. D **106**, 056022 (2022).
[54] G. Janssen, K. Holinde, and J. Speth, Phys. Rev. C **49**, 2763 (1994).
[55] J. L. Lucio-Martinez, M. Napsuciale, M. D. Scadron, and V. M. Villanueva, Phys. Rev. D **61**, 034013 (2000).

[56] R. Casalbuoni, A. Deandrea, N. Di Bartolomeo, R. Gatto, F. Feruglio, and G. Nardulli, Phys. Lett. B **302**, 95 (1993).
[57] F. De Fazio, Phys. Rev. D **79**, 054015 (2009); **83**, 099901(E) (2011).
[58] L. C. Liu, Q. Haider, and J. T. Londergan, Phys. Rev. C **51**, 3427 (1995).
[59] E. Braaten and M. Kusunoki, Phys. Rev. D **72**, 054022 (2005).